WAVE PROPAGATION IN DAMAGED COMPOSITE MATERIALS

Jacob Aboudi†

Department of Engineering Science and Mechanics, Virginia Polytechnic Institute and
State University, Blacksburg, VA 24061, U.S.A.

Abstract—A continuum theory for elastic wave propagation in three-dimensional composite materials with imperfect bonding between the phases is presented. The theory provides the dispersion relations for harmonic wave propagation, and the dynamic response of the composite to impulsive loadings. Long-fiber and periodically bilaminated composites are obtained by a proper selection of some geometrical parameters. Furthermore, perfect contact, perfect lubrication and complete debonding of the constituents are obtained as special cases. The effects of periodic distribution of cracks in solids, and of damage in composite laminates on propagating elastic waves are presented.

1. INTRODUCTION

The determination of the dynamic response of composite materials is very important because they are frequently used in situations involving the sudden application of loads. Methods of analysis of wave propagation in composite materials can be found in the book by Christensen (1979) where an extensive list of references is given.

In a recent publication (Aboudi, 1986) a continuum theory for harmonic wave propagation in three-dimensional composites was presented. By applying this theory, dispersion relations were determined for short-fiber composites, and long-fiber composites and periodically layered media were obtained as special cases. This continuum model has been generalized (Aboudi, 1987a) to predict the dynamic response of composite materials to impulsive loadings. In both papers, the predicted dispersion relations and transient waves were determined solely from the elastic constants of the constituents (assumed in general to be orthotropic), their mass densities and geometrical dimensions. The prediction of the theory was checked by comparison with different approaches in various situations and good agreements were obtained.

In most of the works dealing with wave propagation in composite materials, perfect contact is assumed to exist between the phases. This of course is an idealization of the complex situation where an interphase is known to exist between the constituents. This zone of imperfection incorporates the effect of adsorption, shrinkage due to permanent stresses, voids, flows, microcracks, imperfect adhesion, etc. In fact, the transfer of load which is the principal objective of the reinforcement of weak matrices by high modulus, high strength fibers, depends mainly on good bonding. Thus, although a precise description of the interface between the phases is very complicated, the incorporation of its effect on the behavior of the composite is essential. It should be noted that perfect bonding is a demanding requirement, since it is the desire to weld together materials which by their nature may not be directly welded.

Several attempts appear in the literature which incorporate the effect of imperfect bonding in composites. They mainly consist of the introduction of a third phase between the fiber and matrix constituent. The effect of degree of adhesion is represented by a proper choice of the material constants, mass density and thickness of the interphase. Furthermore, if the interphase is modeled as an inhomogeneous layer (Theocaris and Phillippidis, 1985), then additional assumptions about the specific variation of its elastic moduli are needed.

Rather than adopting the approach of an interphase layer, the simplified model of Jones and Whittier (1967) can be used to represent imperfect bonding between the constituents. They represent the effect of partial adhesion as a thin elastic film the shear stress

---

† On leave from the Faculty of Engineering, Tel-Aviv University, Ramat-Aviv 69978, Israel.

of which is taken to depend on the relative tangential displacement at the interface, whereas the normal bond stress is proportional to the relative normal displacements. Thus, this model of imperfect bonding between the phases consists of two parameters which represent the degree of adhesion in shear and normal at the interfaces.

In this paper the approach of Jones and Whittier (1967) for the modeling of imperfect bonding is incorporated in the theory presented for harmonic and transient waves in composites with perfect contact (Aboudi, 1986, 1987a). The resulting continuum model provides a set of equations from which the phase velocities of harmonic waves propagating in a three-dimensional composite with imperfect bonding between the constituents can be determined. The derived theory can also predict the dynamic response of the composite to impacting loads. Thus, the effect of the degree of adhesion between the phases on propagating waves and pulses can be studied. Perfect contact, perfect lubrication and complete debonding at the interface are obtained as special cases by a proper selection of the two parameters. In its most general form, the theory is formulated for a three-dimensional composite. Long-fiber and periodically bilaminated composites can be obtained by a proper selection of some geometrical parameters. In a recent paper (Aboudi, 1987b) the effective moduli and coefficients of thermal expansion of composite materials were predicted using the above model for interface decohesion.

In addition to the study of the effect of the degree of adhesion between the constituents in the micromechanical analysis, the effect of damage in homogeneous materials can be studied using elastic waves. To this end the derived theory is applied to investigate the effect of a periodic distribution of cracks in solids on elastic wave propagation. Both transient and harmonic wave propagation are studied, where in the latter case the resulting exact dispersion relation, established recently by Achenbach and Li (1986), is utilized for comparison. It should be mentioned that the application of elastic waves for the detection and study of flows in materials is of considerable importance in non-destructive evaluations, see Thompson (1984) for a recent review.

Finally, the present theory is applied to study the influence of damage on propagating waves in composite laminates. It is well known (Highsmith and Reifsnider, 1982) that transverse cracks appear along the fibers in the off-axis plies of the laminate in the first stage of either quasi-static or cyclic loadings. At a later stage, longitudinal cracks are formed along the fibers of the 0° plies (Jamison et al., 1984). The effect of these two systems of cracks on propagating waves in the damaged laminate is studied using the present continuum theory.

2. IMPERFECT BONDING

The effect of imperfect bonding between inclusions and matrix in a composite material may be incorporated by assuming that an interfacial layer exists between the two constituents. Thus, the composite is considered as consisting of three phases, that is the matrix, the inclusions and a third one, which is the zone of imperfections surrounding each one of the inclusions. The thickness and material properties of the interphase can be used to describe the quality of adhesion between the matrix and fiber. The determination of the properties of the inner-phase, which may be heterogeneous, obviously involves many parameters the determination of which may be difficult. This difficulty can be circumvented by adopting the simplified model of Jones and Whittier (1967). The effect of imperfect bonding is represented by these authors as a thin elastic film the shear stress of which is taken to depend on the relative tangential displacement at the interface, whereas the normal bond stress is proportional to the relative normal displacements. This approach is adopted in this paper where a continuum theory is developed for wave propagation in composite materials in which the effect of imperfect bonding between the constituents is incorporated.

In Cartesian coordinates (x_1, x_2, x_3), let u_i and σ_{ij} $(i, j = 1, 2, 3)$ denote the components of the displacement vector and stress tensor, respectively. At interface I between phases 1 and 2 the usual condition of the continuity of the traction vector must be satisfied

$$[\sigma_{ij} n_j]_I = 0 \tag{1}$$

where **n** is the normal vector to I, and $[\cdot]_I$ is the jump of the relevant quantity across I.

According to Jones and Whittier (1967) we have for the jump of the normal displacement across the interface

$$[\mathbf{u}_n]_I = R_n \boldsymbol{\sigma}_n|_I \qquad (2)$$

where

$$\mathbf{u}_n = u_i n_i \mathbf{n}, \quad \boldsymbol{\sigma}_n = (\sigma_{ij} n_i n_j)\mathbf{n}$$

which are, respectively, the normal displacement and traction vectors, and R_n is an appropriate parameter.

Similarly, the jump of the tangential displacement vector at I is given by

$$[\mathbf{u}_t]_I = R_t \boldsymbol{\sigma}_t|_I \qquad (3)$$

where

$$\mathbf{u}_t = \mathbf{u} - \mathbf{u}_n$$

and

$$\boldsymbol{\sigma}_t = \mathbf{t}^{(\mathbf{n})} - \boldsymbol{\sigma}_n$$

are the tangential displacement vector and shear traction vector, respectively. Here $\mathbf{t}^{(\mathbf{n})}$ is the traction vector ($t_i^{(\mathbf{n})} = \sigma_{ij} n_j$) and the corresponding parameter is denoted by R_t. In eqns (2) and (3) R_n and R_t are parameters describing the flexible bond; R_n is equal to the film thickness divided by the Young's modulus of the bond film, and R_t is equal to the film thickness divided by its shear modulus. $R_n \to 0$, $R_t \to 0$ implies perfectly bonded constituents (i.e. perfect contact); $R_n \to 0$, $R_t \to \infty$ perfectly lubricated contact and $R_n \to \infty$ correspond to the case of completely debonded phases.

This model for imperfect bonding is used in the sequel for the study of the effect of the degree of adhesion between the constituents on propagating waves in composites. In the special case of perfect contact, the theory reduces to that given previously (Aboudi, 1986, 1987a).

3. GEOMETRY AND DISPLACEMENT EXPANSION

As previously (Aboudi, 1986), the composite is modeled by rectangular parallelepiped shaped inclusions imbedded regularly in the matrix, forming a triply periodic array in the x_1, x_2 and x_3 directions, see Fig. 1(a). The parameters d_1, h_1, l_1 specify the dimensions of the inclusions, and d_2, h_2, l_2 represent the spacing of the inclusions within the matrix in the three orthogonal directions. Particulate, as well as short-fiber, long-fiber and periodically bilaminated composites are obtained by a proper selection of these parameters. Both fibers and matrix are considered presently to be perfectly elastic anisotropic materials.

Due to the assumed periodic structure it is sufficient to consider a representative cell of dimensions (d_1+d_2), (h_1+h_2), (l_1+l_2) as shown in Fig. 1(b). This cell is identified by the triplet (p, q, r) where p, q, r are running indices in the x_1, x_2, x_3 directions, respectively (e.g. the neighboring cells labeled by (p, q, r) and $(p+1, q, r)$ correspond to the representative cell of Fig. 1(b) and the one located just above it, respectively). The cell is divided into eight subcells α, β, $\gamma = 1, 2$, and eight local systems of coordinates $(\bar{x}_1^{(\alpha)}, \bar{x}_2^{(\beta)}, \bar{x}_3^{(\gamma)})$ are introduced the origins of which are located at the center of each subcell. Their positions are denoted by $x_1^{(\alpha)}$, $x_2^{(\beta)}$ and $x_3^{(\gamma)}$. Here and in the sequel the subscripts or superscripts α, β, γ will indicate that quantities belong to one of the subcells. Repeated α or β or γ does not imply summation.

A high order continuum theory can be developed for modeling the behavior of the composite, which is based on the expansion of the displacement vector at a point in a subcell of the representative cell (p, q, r), in terms of the coordinates of that point with respect to the local system. This expansion can be expressed in terms of the Legendre polynomials permitting the modeling of increasingly complex deformation patterns within the subcell.
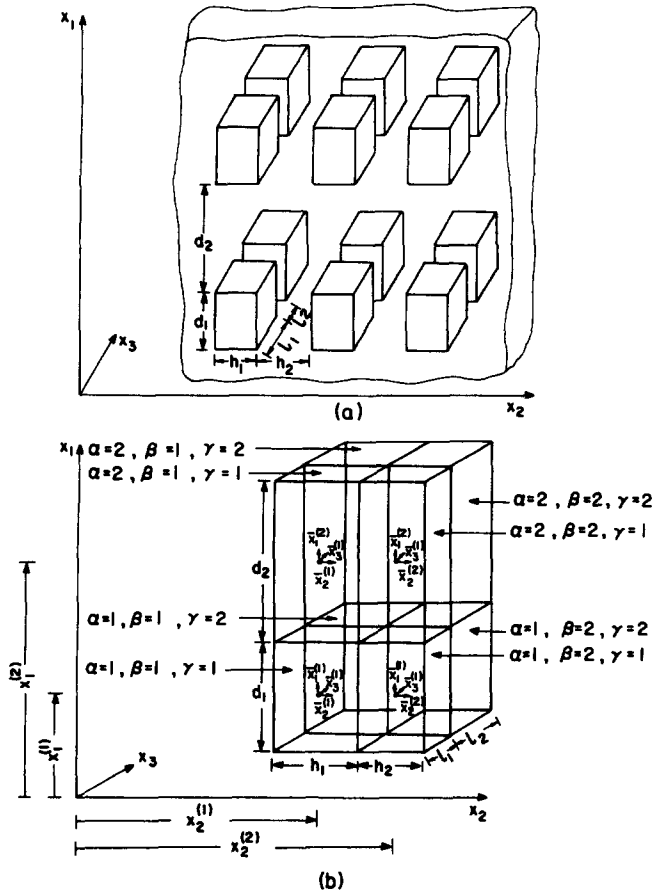
Fig. 1. (a) A composite with rectangular parallelepiped inclusions imbedded in the matrix in a triply periodic array. (b) The representative (p, q, r) cell.

It can be written in the form

$$\mathbf{u}^{(\alpha\beta\gamma)} = \mathbf{w}^{(\alpha\beta\gamma)} + \bar{x}_1^{(\alpha)}\boldsymbol{\phi}^{(\alpha\beta\gamma)} + \bar{x}_2^{(\beta)}\boldsymbol{\chi}^{(\alpha\beta\gamma)} + \bar{x}_3^{(\gamma)}\boldsymbol{\psi}^{(\alpha\beta\gamma)} + \tfrac{1}{2}(\bar{x}_1^{(\alpha)^2} - \tfrac{1}{4}d_\alpha^2)\mathbf{U}^{(\alpha\beta\gamma)} + \tfrac{1}{2}(\bar{x}_2^{(\beta)^2} - \tfrac{1}{4}h_\beta^2)\mathbf{V}^{(\alpha\beta\gamma)}$$

$$+ \tfrac{1}{2}(\bar{x}_3^{(\gamma)^2} - \tfrac{1}{4}l_\gamma^2)\mathbf{W}^{(\alpha\beta\gamma)} + \cdots \tag{4}$$

where $\mathbf{u}^{(\alpha\beta\gamma)}$ is the displacement vector in the subcell $(\alpha\beta\gamma)$ and $\mathbf{w}^{(\alpha\beta\gamma)}$, $\boldsymbol{\phi}^{(\alpha\beta\gamma)}, \ldots,$ are time-dependent functions defined at the discrete points $x_1 = x_1^{(\alpha)}$, $x_2 = x_2^{(\beta)}, x_3 = x_3^{(\gamma)}$. By a smoothing operation the discrete nature of the composite can be eliminated and a homogeneous continuous model is obtained. This is achieved by considering the above functions to be continuously dependent on x_1, x_2, x_3. In this paper the above expansion is confined to a second-order one.

Both dilatational and shear waves can be treated by the present approach. It was decided however to consider in this paper shear wave propagation since the use of shear wave speed, in the transverse direction, to test for debonding seems to be of relevance in nondestructive methods for evaluating composite materials containing damage. Thus for shear waves oriented in the x_2-direction and propagating in the x_1-direction, the following second-order expansion of the displacement is applicable due to symmetry considerations:

$$u_1^{(\alpha\beta\gamma)} = \bar{x}_2^{(\beta)}\chi_1^{(\alpha\beta\gamma)},$$

$$u_2^{(\alpha\beta\gamma)} = w_2^{(\alpha\beta\gamma)} + \bar{x}_1^{(\alpha)}\phi_2^{(\alpha\beta\gamma)} + \tfrac{1}{2}(3\bar{x}_1^{(\alpha)^2} - \tfrac{1}{4}d_\alpha^2)U_2^{(\alpha\beta\gamma)} + \tfrac{1}{2}(3\bar{x}_2^{(\beta)^2} - \tfrac{1}{4}h_\beta^2)V_2^{(\alpha\beta\gamma)} + \tfrac{1}{2}(3\bar{x}_3^{(\gamma)^2} - \tfrac{1}{4}l_\gamma^2)W_2^{(\alpha\beta\gamma)},$$

$$u_3^{(\alpha\beta\gamma)} = 0. \tag{5}$$

Shear waves oriented in the x_3-direction and propagating in the x_1-direction can be obtained from eqns (5) by redefining the geometrical parameters d_α, h_β and l_γ.

The components of the small strain tensor are given by

$$\varepsilon_{ij}^{(\alpha\beta\gamma)} = \tfrac{1}{2}[\partial_i u_j^{(\alpha\beta\gamma)} + \partial_j u_i^{(\alpha\beta\gamma)}], \quad i, j = 1, 2, 3 \tag{6}$$

where $\partial_1 = \partial/\partial\bar{x}_1^{(\alpha)}$, $\partial_2 = \partial/\partial\bar{x}_2^{(\beta)}$ and $\partial_3/\partial\bar{x}_3^{(\gamma)}$.

4. EQUATIONS OF MOTION

It was previously shown (Aboudi, 1986) that by using eqns (5), the dynamic equations of motion in the subcell region $(\alpha\beta\gamma)$ are given by

$$I_{12(0,0,0)}^{(\alpha\beta\gamma)} + J_{22(0,0,0)}^{(\alpha\beta\gamma)} + K_{32(0,0,0)}^{(\alpha\beta\gamma)} = \rho_{\alpha\beta\gamma} \ddot{w}_2^{(\alpha\beta\gamma)} \tag{7}$$

$$I_{12(1,0,0)}^{(\alpha\beta\gamma)} - S_{12(0,0,0)}^{(\alpha\beta\gamma)} = \frac{1}{12} \rho_{\alpha\beta\gamma} d_\alpha^2 \ddot{\phi}_2^{(\alpha\beta\gamma)} \tag{8}$$

$$J_{21(0,1,0)}^{(\alpha\beta\gamma)} - S_{12(0,0,0)}^{(\alpha\beta\gamma)} = \frac{1}{12} \rho_{\alpha\beta\gamma} h_\beta^2 \ddot{\chi}_1^{(\alpha\beta\gamma)} \tag{9}$$

$$3I_{12(0,0,0)}^{(\alpha\beta\gamma)} + J_{22(0,0,0)}^{(\alpha\beta\gamma)} + K_{32(0,0,0)}^{(\alpha\beta\gamma)} - 24S_{12(1,0,0)}^{(\alpha\beta\gamma)}/d_\alpha^2 = \rho_{\alpha\beta\gamma} \left[\ddot{w}_2^{(\alpha\beta\gamma)} + \frac{1}{10} d_\alpha^2 \ddot{U}_2^{(\alpha\beta\gamma)} \right] \tag{10}$$

$$I_{12(0,0,0)}^{(\alpha\beta\gamma)} + 3J_{22(0,0,0)}^{(\alpha\beta\gamma)} + K_{32(0,0,0)}^{(\alpha\beta\gamma)} - 24S_{22(0,1,0)}^{(\alpha\beta\gamma)}/h_\beta^2 = \rho_{\alpha\beta\gamma} \left[\ddot{w}_2^{(\alpha\beta\gamma)} + \frac{1}{10} h_\beta^2 \ddot{V}_2^{(\alpha\beta\gamma)} \right] \tag{11}$$

$$I_{12(0,0,0)}^{(\alpha\beta\gamma)} + J_{22(0,0,0)}^{(\alpha\beta\gamma)} + 3K_{32(0,0,0)}^{(\alpha\beta\gamma)} - 24S_{23(0,0,1)}^{(\alpha\beta\gamma)}/l_\gamma^2 = \rho_{\alpha\beta\gamma} \left[\ddot{w}_2^{(\alpha\beta\gamma)} + \frac{1}{10} l_\gamma^2 \ddot{W}_2^{(\alpha\beta\gamma)} \right] \tag{12}$$

where $\rho_{\alpha\beta\gamma}$ is the mass density of the material occupying the subcell $(\alpha\beta\gamma)$ and dots denote differentiations with respect to time. In addition

$$S_{ij(l,m,n)}^{(\alpha\beta\gamma)} = \frac{1}{v_{\alpha\beta\gamma}} \int_{-d_\alpha/2}^{d_\alpha/2} \int_{-h_\beta/2}^{h_\beta/2} \int_{-l_\gamma/2}^{l_\gamma/2} (\bar{x}_1^{(\alpha)})^l (\bar{x}_2^{(\beta)})^m (\bar{x}_3^{(\gamma)})^n \sigma_{ij}^{(\alpha\beta\gamma)} \, d\bar{x}_1^{(\alpha)} \, d\bar{x}_2^{(\beta)} \, d\bar{x}_3^{(\gamma)}, \quad i, j = 1, 2, 3 \tag{13}$$

where $v_{\alpha\beta\gamma} = d_\alpha h_\beta l_\gamma$. The higher order stresses (13) can be evaluated by using the relevant elastic stress–strain relations which characterize the material occupying the subcell $(\alpha\beta\gamma)$, in conjunction with eqns (6) and (5). The resulting expression gives $S_{ij(l,m,n)}^{(\alpha\beta\gamma)}$ in terms of $\chi_1^{(\alpha\beta\gamma)}$, $w_2^{(\alpha\beta\gamma)}$, $\phi_2^{(\alpha\beta\gamma)}$, U_2, V_2 and W_2.

In eqns (7)–(12)

$$I_{1j(n,0,0)}^{(\alpha\beta\gamma)} = \frac{1}{v_{\alpha\beta\gamma}} \left(\frac{d_\alpha}{2}\right)^n \int_{-h_\beta/2}^{h_\beta/2} \int_{-l_\gamma/2}^{l_\gamma/2} [\sigma_{1j}^{(\alpha\beta\gamma)}(d_\alpha/2) + (-1)^{n+1} \sigma_{1j}^{(\alpha\beta\gamma)}(-d_\alpha/2)] \, d\bar{x}_2^{(\beta)} \, d\bar{x}_3^{(\gamma)} \tag{14}$$

$$J_{2j(0,n,0)}^{(\alpha\beta\gamma)} = \frac{1}{v_{\alpha\beta\gamma}} \left(\frac{h_\beta}{2}\right)^n \int_{-d_\alpha/2}^{d_\alpha/2} \int_{-l_\gamma/2}^{l_\gamma/2} [\sigma_{2j}^{(\alpha\beta\gamma)}(h_\beta/2) + (-1)^{n+1} \sigma_{2j}^{(\alpha\beta\gamma)}(-h_\beta/2)] \, d\bar{x}_2^{(\alpha)} \, d\bar{x}_3^{(\gamma)} \tag{15}$$

$$K_{3j(0,0,n)}^{(\alpha\beta\gamma)} = \frac{1}{v_{\alpha\beta\gamma}} \left(\frac{l_\gamma}{2}\right)^n \int_{-d_\alpha/2}^{d_\alpha/2} \int_{-h_\beta/2}^{h_\beta/2} [\sigma_{3j}^{(\alpha\beta\gamma)}(l_\gamma/2) + (-1)^{n+1} \sigma_{3j}^{(\alpha\beta\gamma)}(-l_\gamma/2)] \, d\bar{x}_1^{(\alpha)} \, d\bar{x}_2^{(\beta)} \tag{16}$$

where $\sigma_{1j}^{(\alpha\beta\gamma)}(\pm d_\alpha/2), \sigma_{2j}^{(\alpha\beta\gamma)}(\pm h_\beta/2)$, $\sigma_{3j}^{(\alpha\beta\gamma)}(\pm l_\gamma/2)$ stand for the interfacial stresses at $\bar{x}_1^{(\alpha)} = \pm d_\alpha/2, \bar{x}_2^{(\beta)} = \pm h_\beta/2, \bar{x}_3^{(\gamma)} = \pm l_\gamma/2$, respectively.

The system of eqns (7)–(12) forms the dynamic equations for shear waves propagating in the x_1-direction and oriented in the x_2-direction, in the framework of a second-order theory. In these equations the expressions involving the interfacial stresses are unknown quantities which will be determined by using the relevant continuity conditions of the tractions at the interfaces between the subcells of the representative cell of Fig. 1(b), and at the interfaces between neighboring cells.

5. TRACTION CONTINUITY CONDITIONS

At the interfaces of the subcells of the representative cell (p, q, r) of Fig. 1(b), the tractions must be continuous, i.e.

$$\sigma_{1i}^{(1\beta\gamma)}\big|_{\bar{x}_1^{(1)} = d_1/2} = \sigma_{1i}^{(2\beta\gamma)}\big|_{\bar{x}_1^{(2)} = -d_2/2} \tag{17}$$

$$\sigma_{2i}^{(\alpha 1\gamma)}\big|_{\bar{x}_2^{(1)} = h_1/2} = \sigma_{2i}^{(\alpha 2\gamma)}\big|_{\bar{x}_2^{(2)} = -h_2/2} \tag{18}$$

$$\sigma_{3i}^{(\alpha\beta 1)}\big|_{\bar{x}_3^{(1)} = l_1/2} = \sigma_{3i}^{(\alpha\beta 2)}\big|_{\bar{x}_3^{(2)} = -l_2/2}. \tag{19}$$

Further, the continuity of tractions between neighboring cells must also be ensured. These are given by the following relations:

$$\sigma_{1i}^{(1\beta\gamma)}\big|_{\bar{x}_1^{(1)} = -d_1/2}^{(p+1,q,r)} = \sigma_{1i}^{(2\beta\gamma)}\big|_{\bar{x}_1^{(2)} = d_2/2} \tag{20}$$

$$\sigma_{2i}^{(\alpha 1\gamma)}\big|_{\bar{x}_2^{(1)} = -h_1/2}^{(p,q+1,r)} = \sigma_{2i}^{(\alpha 2\gamma)}\big|_{\bar{x}_2^{(2)} = h_2/2} \tag{21}$$

$$\sigma_{3i}^{(\alpha\beta 1)}\big|_{\bar{x}_3^{(1)} = -l_1/2}^{(p,q,r+1)} = \sigma_{3i}^{(\alpha\beta 2)}\big|_{\bar{x}_3^{(2)} = l_2/2}. \tag{22}$$

In order to facilitate the notations, all quantities belonging to the cell (p, q, r) will appear (as in eqns (17)–(19)) without the superindices (p, q, r).

The above continuity conditions (17)–(22) imply relationships between the quantities defined in eqns (14)–(16). In establishing these relations, let us define

$$F_{ij}^{(1\beta\gamma)} = \sigma_{ij}^{(1\beta\gamma)}\big|_{d_1/2} - \sigma_{ij}^{(1\beta\gamma)}\big|_{-d_1/2} \tag{23}$$

and

$$G_{ij}^{(1\beta\gamma)} = \sigma_{ij}^{(1\beta\gamma)}\big|_{d_1/2} + \sigma_{ij}^{(1\beta\gamma)}\big|_{-d_1/2}. \tag{24}$$

Using eqns (17) and (20) we have

$$F_{12}^{(1\beta\gamma)} = \sigma_{12}^{(2\beta\gamma)}\big|_{-d_2/2} - \sigma_{12}^{(2\beta\gamma)}\big|_{d_2/2}^{(p-1,q,r)} \tag{25}$$

and

$$G_{12}^{(1\beta\gamma)} = \sigma_{12}^{(2\beta\gamma)}\big|_{-d_2/2} + \sigma_{12}^{(2\beta\gamma)}\big|_{d_2/2}^{(p-1,q,r)}. \tag{26}$$

By addition and subtraction of equal quantities to eqns (25) and (26) it can be easily verified that

$$2F_{12}^{(1\beta\gamma)} = -F_{12}^{(2\beta\gamma)} + G_{12}^{(2\beta\gamma)} - [F_{12}^{(2\beta\gamma)} + G_{12}^{(2\beta\gamma)}]^{(p-1,q,r)} \tag{27}$$

and

$$2G_{12}^{(1\beta\gamma)} = G_{12}^{(2\beta\gamma)} - F_{12}^{(2\beta\gamma)} + [G_{12}^{(2\beta\gamma)} + F_{12}^{(2\beta\gamma)}]^{(p-1,q,r)}. \tag{28}$$

Using eqns (27) and (28) in eqn (14) with $j = 1$ we obtain the corresponding relations

$$d_1 I_{12(0,0,0)}^{(1\beta\gamma)} = I_{12(1,0,0)}^{(2\beta\gamma)} - d_2 I_{12(0,0,0)}^{(2\beta\gamma)}/2 - [I_{12(1,0,0)}^{(2\beta\gamma)} + d_2 I_{12(0,0,0)}^{(2\beta\gamma)}/2]^{(p-1,q,r)} \tag{29}$$

$$I_{12(1,0,0)}^{(1\beta\gamma)} = I_{12(1,0,0)}^{(2\beta\gamma)}/2 - d_2 I_{12(0,0,0)}^{(2\beta\gamma)}/4 + \tfrac{1}{2}[I_{12(1,0,0)}^{(2\beta\gamma)} + d_2 I_{12(0,0,0)}^{(2\beta\gamma)}/2]^{(p-1,q,r)}. \tag{30}$$

From eqns (18) and (15) we have

$$J_{21(0,1,0)}^{(\alpha 1\gamma)} = J_{21(0,1,0)}^{(\alpha 2\gamma)} \tag{31}$$

and

$$h_1 J_{22(0,0,0)}^{(\alpha 1\gamma)} = -h_2 J_{22(0,0,0)}^{(\alpha 2\gamma)}. \tag{32}$$

From eqns (19) and (16) we have

$$l_1 K_{32(0,0,0)}^{(\alpha\beta 1)} = -l_2 K_{32(0,0,0)}^{(\alpha\beta 2)}. \tag{33}$$

The other continuity relations are identically satisfied in the present case of an S-wave propagating in the x_1-direction.

Equations (29)–(33) are 20 relations which arise from the traction continuity conditions between subcells and between neighboring cells.

6. DISPLACEMENT INTERFACIAL RELATIONS

Consider the representative cell of Fig. 1(b) which is labeled by the triplecet (p, q, r). Imposing the imperfect bonding conditions for the normal and tangential displacements (2) and (3) at the interface $\bar{x}_1^{(1)} = d_1/2$ between the subcells $(1\beta\gamma)$ and $(2\beta\gamma)$ on the average basis gives

$$\frac{1}{h_\beta l_\gamma} \int_{-h_\beta/2}^{h_\beta/2} \int_{-l_\gamma/2}^{l_\gamma/2} [u_i^{(1\beta\gamma)}|_{\bar{x}_1^{(1)} = d_1/2} - u_i^{(2\beta\gamma)}|_{\bar{x}_1^{(2)} = -d_2/2}] \, d\bar{x}_2^{(\beta)} \, d\bar{x}_3^{(\gamma)}$$

$$= -\frac{1}{h_\beta l_\gamma} R_{1i}^{(\beta\gamma)} \int_{-h_\beta/2}^{h_\beta/2} \int_{-l_\gamma/2}^{l_\gamma/2} \sigma_{1i}^{(1\beta\gamma)}|_{\bar{x}_1^{(1)} = d_1/2} \, d\bar{x}_2^{(\beta)} \, d\bar{x}_3^{(\gamma)} \quad (34)$$

where i is not summed and

$$R_{1i}^{(\beta\gamma)} = \begin{cases} R_n & i = 1 \\ R_t & i = 2, 3. \end{cases} \tag{35}$$

If imperfect bonding, for example, exists between the inclusion $\alpha = \beta = \gamma = 1$ and the surrounding matrix only, we would have that $R_{1i}^{(11)} \neq 0$ and all other $R_{1i}^{(\beta\gamma)}$ are zero. The minus sign on the right-hand side of eqn (34) is introduced to ensure that positive (negative) relative displacements are associated with positive (negative) interfacial stresses.

Substituting eqns (5) in eqn (34) yields for $i = 2$

$$w_2^{(1\beta\gamma)} + \frac{d_1}{2}\phi_2^{(1\beta\gamma)} + \frac{d_1^2}{4}U_2^{(1\beta\gamma)} - w_2^{(2\beta\gamma)} + \frac{d_2}{2}\phi_2^{(2\beta\gamma)} - \frac{d_2^2}{4}U_2^{(2\beta\gamma)}$$

$$= -R_{12}^{(\beta\gamma)}\left[\frac{d_1}{2}I_{12(0,0,0)}^{(1\beta\gamma)} + I_{12(1,0,0)}^{(1\beta\gamma)}\right]$$

$$= R_{12}^{(\beta\gamma)}\left[\frac{d_2}{2}I_{12(0,0,0)}^{(2\beta\gamma)} - I_{12(1,0,0)}^{(2\beta\gamma)}\right] \tag{36}$$

where the last equality was established by using eqns (29) and (30).

A similar relation can be deduced when the imperfect bonding between the representative cell (p, q, r) and its neighboring cell $(p+1, q, r)$ (just above (p, q, r) in the x_1-direction) is imposed. The result is

$$w_2^{(2\beta\gamma)} + \frac{d_2}{2}\phi_2^{(2\beta\gamma)} + \frac{d_2^2}{4}U_2^{(2\beta\gamma)} - \left[w_2^{(1\beta\gamma)} - \frac{d_1}{2}\phi_2^{(1\beta\gamma)} + \frac{d_1^2}{4}U_2^{(1\beta\gamma)}\right]^{(p+1,q,r)}$$

$$= -R_{12}^{(\beta\gamma)}\left[\frac{d_2}{2}I_{12(0,0)}^{(2\beta\gamma)} + I_{12(1,0,0)}^{(2\beta\gamma)}\right]. \tag{37}$$

For the interfacial conditions in the x_2- and x_3-directions we obtain, respectively

$$w_2^{(\alpha 1\gamma)} + \frac{h_1^2}{4}V_2^{(\alpha 1\gamma)} - w_2^{(\alpha 2\gamma)} - \frac{h_2^2}{4}V_2^{(\alpha 2\gamma)} = -R_{22}^{(\alpha\gamma)}\frac{h_1}{2}J_{22(0,0,0)}^{(\alpha 1\gamma)} \tag{38}$$

$$w_2^{(\alpha\beta 1)} + \frac{l_1^2}{4}W_2^{(\alpha\beta 1)} - w_2^{(\alpha\beta 2)} - \frac{l_2^2}{4}W_2^{(\alpha\beta 2)} = -R_{32}^{(\alpha\beta)}\frac{l_1}{2}K_{32(0,0,0)}^{(\alpha\beta 1)}. \tag{39}$$

Finally, the interfacial imperfect bonding condition of the $u_1^{(\alpha\beta\gamma)}$ displacement components provides the following relation:

$$h_1\chi_1^{(\alpha 1\gamma)} + h_2\chi_1^{(\alpha 2\gamma)} = -R_{21}^{(\alpha\beta)}J_{21(0,1,0)}^{(\alpha 1\gamma)}. \tag{40}$$

In eqns (38)–(40)

$$R_{2i}^{(\alpha\gamma)} = \begin{cases} R_n & i = 2 \\ R_t & i = 1, 3 \end{cases} \tag{41}$$

$$R_{3i}^{(\alpha\beta)} = \begin{cases} R_n & i = 3 \\ R_t & i = 1, 2. \end{cases} \tag{42}$$

For example, if imperfect bonding in normal and shear exists between the inclusion $(\alpha = \beta = \gamma = 1)$ and the matrix (α, β, γ), with $\alpha + \beta + \gamma \neq 3$, we have the non-vanishing coefficients $R_{1i}^{(11)} \neq 0$, $R_{2i}^{(11)} \neq 0$ and $R_{3i}^{(11)} \neq 0$. In the special case of perfect bonding between all the interfaces, all the coefficients vanish and eqns (36)–(40) reduce to the corresponding relations obtained in the case of perfect contact (Aboudi, 1986, 1987a) where all displacements are continuous across the interfaces. Equations (36)–(40) are 20 relations for the interfacial conditions between the displacements.

7. GOVERNING EQUATIONS

In this section we establish the equations of motion at interior points of the composite. For harmonic shear wave propagation, these equations are sufficient for the derivation of the frequency equation and the determination of the corresponding dispersion relations. For transient waves, however, the appropriate initial and boundary conditions must be established as well.

In considering the problem of a propagation S-pulse in the x_1-direction in the composite, suppose that the composite material occupies the region $0 \leqslant x_1 \leqslant D$, $|x_2| < \infty$, $|x_3| < \infty$. Let M denote the number of cells along the interval $0 \leqslant x_1 \leqslant D$, i.e. $M = D/(d_1 + d_2)$. These cells are numbered by $p = 1, 2, \ldots, m$. They consist of $p = 2, \ldots, M-1$ internal cells and two boundary cells $p = 0$ and M.

7.1. Interior cells

Substituting eqn (7) in eqn (11) gives

$$\tfrac{1}{6} h_\beta^2 J_{22(0,0,0)}^{(\alpha\beta\gamma)} = Y^{(\alpha\beta\gamma)} \tag{43}$$

where

$$Y^{(\alpha\beta\gamma)} = \rho_{\alpha\beta\gamma} \frac{h_\beta^4}{120} \ddot{V}_2^{(\alpha\beta\gamma)} + 2S_{22(0,1,0)}^{(\alpha\beta\gamma)}. \tag{44}$$

Substituting eqn (7) in eqn (12) gives, similarly

$$\tfrac{1}{6} l_\gamma^2 K_{32(0,0,0)}^{(\alpha\beta\gamma)} = Z^{(\alpha\beta\gamma)} \tag{45}$$

where

$$Z^{(\alpha\beta\gamma)} = \rho_{\alpha\beta\gamma} \frac{l_\gamma^4}{120} \ddot{W}_2 + 2S_{23(0,0,1)}^{(\alpha\beta\gamma)}. \tag{46}$$

Substituting eqn (7) in eqn (10) and using eqns (43) and (45) provides

$$\rho_{\alpha\beta\gamma} \frac{d_\alpha^2}{6} \ddot{w}_2^{(\alpha\beta\gamma)} - 2S_{12(1,0,0)}^{(\alpha\beta\gamma)} - \left(\frac{d_\alpha}{h_\beta}\right)^2 Y^{(\alpha\beta\gamma)} - \left(\frac{d_\alpha}{l_\gamma}\right)^2 Z^{(\alpha\beta\gamma)} = \rho_{\alpha\beta\gamma} \frac{d_\alpha^4}{120} \ddot{U}_2^{(\alpha\beta\gamma)}. \tag{47}$$

By using eqn (43) in eqn (32) we obtain

$$h_2 Y^{(\alpha 1\gamma)} + h_1 Y^{(\alpha 2\gamma)} = 0. \tag{48}$$

Similarly, using eqn (45) in eqn (33) gives

$$l_2 Z^{(\alpha\beta 1)} + l_1 Z^{(\alpha\beta 2)} = 0. \tag{49}$$

From eqns (9) and (31) we have

$$\rho_{\alpha 1\gamma} h_1^2 \ddot{\chi}_2^{(\alpha 1\gamma)} + 12 S_{12(0,0,0)}^{(\alpha 1\gamma)} = \rho_{\alpha 2\gamma} h_2^2 \ddot{\chi}_1^{(\alpha 2\gamma)} + 12 S_{12(0,0,0)}^{(\alpha 2\gamma)}. \tag{50}$$

From eqns (7), (43) and (45) we have the following expression for $I_{12(0,0,0)}^{(\alpha\beta\gamma)}$:

$$I_{12(0,0,0)}^{(\alpha\beta\gamma)} = \rho_{\alpha\beta\gamma} \ddot{w}_2^{(\alpha\beta\gamma)} - \frac{6}{h_\beta^2} Y^{(\alpha\beta\gamma)} - \frac{6}{l_\gamma^2} Z^{(\alpha\beta\gamma)}. \tag{51}$$

Using this expression for $I_{12(0,0,0)}^{(\alpha\beta\gamma)}$ and the expression of $I_{12(1,0,0)}^{(\alpha\beta\gamma)}$ provided by eqn (8) in the continuity relations (29), we obtain

$$\rho_{1\beta\gamma} \ddot{w}_2^{(1\beta\gamma)} - \frac{6}{h_\beta^2} Y^{(1\beta\gamma)} - \frac{6}{l_\gamma^2} Z^{(1\beta\gamma)} + \frac{d_2}{2d_1} \rho_{2\beta\gamma} [\ddot{w}_2^{(2\beta\gamma)} + \ddot{w}_2^{(2\beta\gamma)} |^{(p-1,q,r)}]$$

$$- \frac{3d_2}{d_1 h_\beta^2} [Y^{(2\beta\gamma)} + Y^{(2\beta\gamma)} |^{(p-1,q,r)}] - \frac{3d_2}{d_1 l_\gamma^2} [Z^{(2\beta\gamma)} + Z^{(2\beta\gamma)} |^{(p-1,q,r)}]$$

$$- \frac{1}{d_1} [X^{(2\beta\gamma)} - X^{(2\beta\gamma)} |^{(p-1,q,r)}] = 0 \tag{52}$$

where

$$X^{(\alpha\beta\gamma)} = \rho_{\alpha\beta\gamma} \frac{d_\alpha^2}{12} \ddot{\phi}_2^{(\alpha\beta\gamma)} + S^{(\alpha\beta\gamma)}_{12(0,0,0)}.$$

If, on the other hand, the continuity relations (30) are used, the following equations result:

$$X^{(1\beta\gamma)} - \tfrac{1}{2}[X^{(2\beta\gamma)} + X^{(2\beta\gamma)}|^{(p-1,q,r)}] + \frac{d_2}{4}\rho_{2\beta\gamma}[\ddot{w}_2^{(2\beta\gamma)} - \ddot{w}_2^{(2\beta\gamma)}|^{(p-1,q,r)}]$$

$$- \frac{3d_2}{2h_\beta^2}[Y^{(2\beta\gamma)} - Y^{(2\beta\gamma)}|^{(p-1,q,r)}] - \frac{3d_2}{2l_\gamma^2}[Z^{(2\beta\gamma)} - Z^{(2\beta\gamma)}|^{(p-1,q,r)}] = 0. \quad (53)$$

Equations (47)–(50), (52) and (53) are the dynamic equations of motion in conjunction with the traction continuity conditions. The displacement interfacial relations (36)–(40) can be rewritten, based on the above development, in the form

$$w_2^{(1\beta\gamma)} + \frac{d_1}{2}\phi_2^{(1\beta\gamma)} + \frac{d_1^2}{4}U_2^{(1\beta\gamma)} - w_2^{(2\beta\gamma)} + \frac{d_2}{4}\phi_2^{(2\beta\gamma)} - \frac{d_2^2}{4}U_2^{(2\beta\gamma)}$$

$$= R_{12}^{(\beta\gamma)}\frac{d_2}{2}\left[\rho_{2\beta\gamma}\ddot{w}_2^{(2\beta\gamma)} - \frac{6}{h_\beta^2}Y^{(2\beta\gamma)} - \frac{6}{l_\gamma^2}Z^{(2\beta\gamma)}\right] - R_{12}^{(\beta\gamma)}X^{(2\beta\gamma)} \quad (54)$$

$$w_2^{(2\beta\gamma)} + \frac{d_2}{2}\phi_2^{(2\beta\gamma)} + \frac{d_2^2}{4}U_2^{(2\beta\gamma)} - \left[w_2^{(1\beta\gamma)} - \frac{d_1}{2}\phi_2^{(1\beta\gamma)} + \frac{d_1^4}{4}U_2^{(1\beta\gamma)}\right]^{(p+1,q,r)}$$

$$= -R_{12}^{(\beta\gamma)}\frac{d_2}{2}\left[\rho_{2\beta\gamma}\ddot{w}_2^{(2\beta\gamma)} - \frac{6}{h_\beta^2}Y^{(2\beta\gamma)} - \frac{6}{l_\gamma^2}Z^{(2\beta\gamma)}\right] - R_{12}^{(\beta\gamma)}X^{(2\beta\gamma)} \quad (55)$$

$$w_2^{(\alpha 1\gamma)} + \frac{h_1^2}{4}V_2^{(\alpha 1\gamma)} - w_2^{(\alpha 2\gamma)} - \frac{h_2^2}{4}V_2^{(\alpha 2\gamma)} = -\frac{3}{h_1}R_{22}^{(\alpha\gamma)}Y^{(\alpha 1\gamma)} \quad (56)$$

$$w_2^{(\alpha\beta 1)} + \frac{l_1^2}{4}W_2^{(\alpha\beta 1)} - w_2^{(\alpha\beta 2)} - \frac{l_2^2}{4}W_2^{(\alpha\beta 2)} = -\frac{3}{l_1}R_{32}^{(\alpha\beta)}Z^{(\alpha\beta 1)} \quad (57)$$

$$h_1\chi_1^{(\alpha 1\gamma)} + h_2\chi_1^{(\alpha 2\gamma)} = -R_{21}^{(\alpha\gamma)}\left[\rho_{\alpha 1\gamma}\frac{h_1^2}{12}\ddot{\chi}_1^{(\alpha 1\gamma)} + S^{(\alpha 1\gamma)}_{12(0,0,0)}\right] \quad (58)$$

respectively.

Equations (47)–(50), (52) and (53) together with the 20 interfacial displacement relations (54)–(58) form altogether 48 equations which govern the motion at any interior cell $(\alpha\beta\gamma)$. The 48 unknowns are the second-order time derivatives of the field microvariables which appear on the right-hand side of eqns (5).

7.2. Boundary cells

For the boundary cells $p = 1$ and M different treatment should be adopted. For $p = 1$ the governing equations (47)–(50) and (54)–(58) are operative. Relations (52) and (53), on the other hand, which follow from the continuity of tractions between the cells and neighboring cells are not applicable. They are replaced by the conditions of continuity of tractions at the cell $(p = 1)$ interior interfaces (17), and the applied stress loading

$$\bar{\sigma}_{12}^{(1\beta\gamma)} = f(t), \quad \bar{x}_1^{(1)} = -d_1/2 \quad (59)$$

with $f(t)$ describing the temporal variation of this loading. At the other boundary cell

$p = M$, the previously derived governing equations are operative except relations (55) which are obviously not applicable. They are replaced by the condition that the surface $x_1 = D$ is stress free (say) which implies that

$$\sigma_{12}^{(2\beta\gamma)} = 0, \quad \bar{x}_1^{(2)} = d_2/2. \tag{60}$$

For other types of boundary conditions, eqns (60) should be modified accordingly.

The governing equations at interior and boundary cells form a system of $48M$ linear ordinary differential equations in the field microvariables of the cells along $0 \leqslant x_1 \leqslant D$. This system can be represented in the form

$$\mathbf{A\ddot{Q}} + \mathbf{BQ} = \mathbf{D} \tag{61}$$

where $\mathbf{A}$ and $\mathbf{B}$ are constant matrices, $\mathbf{D}$ is a time-dependent vector and $\mathbf{Q}$ is the vector of unknowns. The solution of eqn (61) can be easily obtained by any standard stable procedure in time, utilizing the band structure of $\mathbf{A}$ and $\mathbf{B}$.

8. APPLICATIONS

The previously derived continuum theory is applied here in order to determine the dispersion relations for harmonic waves in composite materials with imperfect bonding, and their response to impact loadings given by eqns (59).

The elastic stress–strain relations of the constituents of the two-phase composite of Fig. 1(a) are taken to be orthotropic. Accordingly

$$\sigma^{(\alpha\beta\gamma)} = \mathbf{C}^{(\alpha\beta\gamma)}\varepsilon^{(\alpha\beta\gamma)} \tag{62}$$

where

$$\sigma^{(\alpha\beta\gamma)} = [\sigma_{11}^{(\alpha\beta\gamma)}, \sigma_{22}^{(\alpha\beta\gamma)}, \sigma_{33}^{(\alpha\beta\gamma)}, \sigma_{12}^{(\alpha\beta\gamma)}, \sigma_{13}^{(\alpha\beta\gamma)}, \sigma_{23}^{(\alpha\beta\gamma)}] \tag{63a}$$

$$\varepsilon^{(\alpha\beta\gamma)} = [\varepsilon_{11}^{(\alpha\beta\gamma)}, \varepsilon_{22}^{(\alpha\beta\gamma)}, \varepsilon_{33}^{(\alpha\beta\gamma)}, 2\varepsilon_{12}^{(\alpha\beta\gamma)}, 2\varepsilon_{13}^{(\alpha\beta\gamma)}, 2\varepsilon_{23}^{(\alpha\beta\gamma)}] \tag{63b}$$

and

$$\mathbf{C}^{(\alpha\beta\gamma)} = \begin{bmatrix} c_{11}^{(\alpha\beta\gamma)} & c_{12}^{(\alpha\beta\gamma)} & c_{13}^{(\alpha\beta\gamma)} & 0 & 0 & 0 \\ & c_{22}^{(\alpha\beta\gamma)} & c_{23}^{(\alpha\beta\gamma)} & 0 & 0 & 0 \\ & & c_{33}^{(\alpha\beta\gamma)} & 0 & 0 & 0 \\ \text{symmetric} & & & c_{44}^{(\alpha\beta\gamma)} & 0 & 0 \\ & & & & c_{55}^{(\alpha\beta\gamma)} & 0 \\ & & & & & c_{66}^{(\alpha\beta\gamma)} \end{bmatrix}. \tag{64}$$

For the isotropic phase

$$c_{11}^{(\alpha\beta\gamma)} = c_{22}^{(\alpha\beta\gamma)} = c_{33}^{(\alpha\beta\gamma)} = \lambda_{\alpha\beta\gamma} + 2\mu_{\alpha\beta\gamma}$$

$$c_{12}^{(\alpha\beta\gamma)} = c_{13}^{(\alpha\beta\gamma)} = c_{23}^{(\alpha\beta\gamma)} = \lambda_{\alpha\beta\gamma} \tag{65}$$

$$c_{44}^{(\alpha\beta\gamma)} = c_{55}^{(\alpha\beta\gamma)} = c_{66}^{(\alpha\beta\gamma)} = \mu_{\alpha\beta\gamma}$$

where $\lambda_{\alpha\beta\gamma}$, $\mu_{\alpha\beta\gamma}$ are the Lamé constants of the phase.

For a transversely isotropic phase for which the axis of anisotropy is in the x_1-direction

$$c_{11}^{(\alpha\beta\gamma)} = E_A^{(\alpha\beta\gamma)} + 4\kappa^{(\alpha\beta\gamma)} [v_A^{(\alpha\beta\gamma)}]^2$$

$$c_{12}^{(\alpha\beta\gamma)} = c_{13}^{(\alpha\beta\gamma)} = 2\kappa^{(\alpha\beta\gamma)} v_A^{(\alpha\beta\gamma)}$$

$$c_{22}^{(\alpha\beta\gamma)} = c_{33}^{(\alpha\beta\gamma)} = \kappa^{(\alpha\beta\gamma)} + G_T^{(\alpha\beta\gamma)} \qquad (66)$$

$$c_{23}^{(\alpha\beta\gamma)} = \kappa^{(\alpha\beta\gamma)} - G_T^{(\alpha\beta\gamma)}$$

$$c_{44}^{(\alpha\beta\gamma)} = c_{55}^{(\alpha\beta\gamma)} = G_A^{(\alpha\beta\gamma)}$$

$$c_{66}^{(\alpha\beta\gamma)} = G_T^{(\alpha\beta\gamma)}$$

where

$$\kappa^{(\alpha\beta\gamma)} = 0.25 E_A^{(\alpha\beta\gamma)}/[0.5(1 - v_T^{(\alpha\beta\gamma)}) (E_A^{(\alpha\beta\gamma)}/E_T^{(\alpha\beta\gamma)}) - (v_A^{(\alpha\beta\gamma)})^2]$$

and

$$G_T^{(\alpha\beta\gamma)} = 0.5 E_T^{(\alpha\beta\gamma)}/(1 + v_T^{(\alpha\beta\gamma)}).$$

In the above equations $E_A^{(\alpha\beta\gamma)}, v_A^{(\alpha\beta\gamma)}$ are the axial Young's modulus and Poisson's ratio, $G_A^{(\alpha\beta\gamma)}$ is the axial shear modulus, and $E_T^{(\alpha\beta\gamma)}, v_T^{(\alpha\beta\gamma)}$ are respectively, the transverse Young's modulus and Poisson's ratio of the material. For transversely isotropic materials with axis of anisotropy oriented in the x_2- or x_3-directions, relations (66) have to be modified accordingly.

The stress moments $S_{ij(l,m,n)}^{(\alpha\beta\gamma)}$ are obtained by substituting eqn (62) in eqn (13) and using eqn (6). The resulting expressions are

$$S_{12(0,0,0)}^{(\alpha\beta\gamma)} = c_{44}^{(\alpha\beta\gamma)} (\chi_1^{(\alpha\beta\gamma)} + \phi_2^{(\alpha\beta\gamma)})$$

$$S_{12(1,0,0)}^{(\alpha\beta\gamma)} = \frac{c_{44}^{(\alpha\beta\gamma)}}{4} d_\alpha^2 U_2^{(\alpha\beta\gamma)}$$

$$S_{22(0,1,0)}^{(\alpha\beta\gamma)} = \frac{c_{22}^{(\alpha\beta\gamma)}}{4} h_\beta^2 V_2^{(\alpha\beta\gamma)} \qquad (67)$$

$$S_{23(0,0,1)}^{(\alpha\beta\gamma)} = \frac{c_{66}^{(\alpha\beta\gamma)}}{4} l_\gamma^2 W_2^{(\alpha\beta\gamma)}.$$

Suppose that the stress loading, eqns (59), is chosen in the form of a semi-infinite impulse of a unit amplitude. In this case the time-dependent function $f(t)$ can be taken as $f(t) = \ddot{g}(t)$, where

$$g(t) = [t^3 H(t) - 3(t-\Delta)^3 H(t-\Delta) + 3(t-2\Delta)^3 H(t-2\Delta) - (t-3\Delta)^3 H(t-3\Delta)]/(6\Delta^3) \quad (68)$$

$H(t)$ is the Heaviside step function and Δ is a parameter. It can be easily verified that $g(t)$ describes a curve which rises smoothly from $g(0) = 0$ to $g(3\Delta) = 1$, and $g(t) = 1$ for $t \geqslant 3\Delta$. For $\Delta \to 0$, $g(t)$ approaches the Heaviside step function which describes the requested unit semi-infinite impulse.

When the dispersion relations of the composite are sought, any one of the 48 microvariables in eqns (47)–(50), (52)–(58) is represented in the form

$$A = \bar{A} \exp [i(kx_1 - \omega t)] \qquad (69)$$

where $\bar{A}$ is an amplitude factor, k is the wave number, ω is the circular frequency and i is the imaginary unit. The phase velocity is given by $c = \omega/k$. Any variable $A^{(p \mp 1, q, r)}$, for example, in the cell $(p \mp 1, q, r)$ is related to A in the cell (p, q, r) by (Aboudi, 1986)
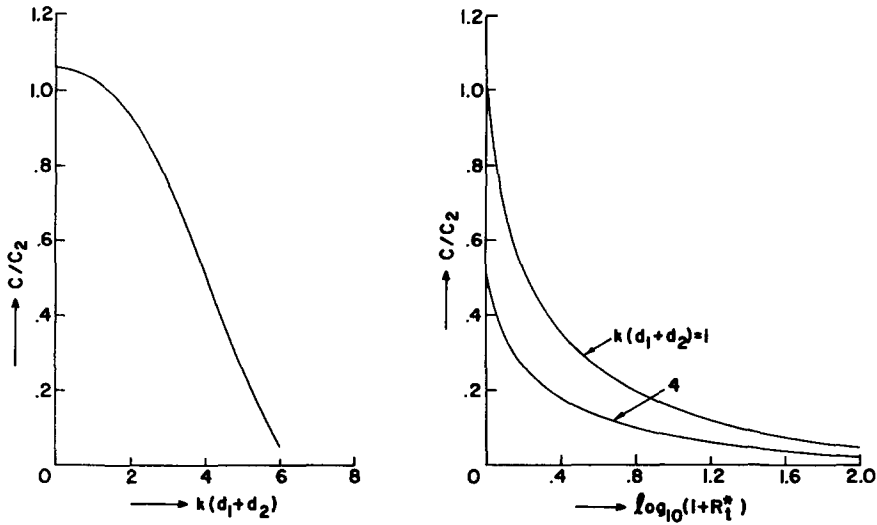
Fig. 2. Phase velocity c/c_2 (c_2 is the shear wave speed in layer 2) against wave number k for propagating shear waves normal to the layering of laminated composite of alternating layers characterized by eqns (71) with perfect contact (left). Reduction of phase velocity with imperfect bonding in shear parameter $R_t^* = R_t \mu_2/(d_1 + d_2)$ (right). In all cases the present prediction coincides with the exact solution given in the Appendix.

$$A^{(p \mp 1, q, r)} = A \exp (\mp i\xi) \tag{70}$$

where $\xi = k(d_1 + d_2)$. A system of 48 homogeneous equations is obtained, and the frequency equation is established by equating the corresponding determinant to zero. This provides a non-linear transcendental equation between the phase velocity and wave number.

8.1. Harmonic wave propagation normal to the layering

In the special case of $h_1/h_2 \to \infty$ and $l_1/l_2 \to \infty$, a periodically bilaminated composite is obtained in which d_1 and d_2 stand for the widths of layers. Shear waves propagating in the x_1-direction imply wave propagation normal to the layering (Fig. 1(a)).

For isotropic layers, the exact frequency equation for a laminated medium with perfect contact between the layers is given by eqn (99) from Sun et al. (1968) for shear waves. For layers with imperfect bonding, the exact frequency equation is given in the Appendix. The latter is used to check the validity of the dispersion curves as predicted by the present theory in this special case.

Results are given for a laminated composite which consists of isotropic layers characterized by

$$d_1/d_2 = 1.5, \quad \rho_1/\rho_2 = 3, \quad \mu_1/\mu_2 = 100 \tag{71}$$

where subindices 1 and 2 denote the various quantities in the two layers (ρ stands for the mass density and μ for the rigidity). In Fig. 2, phase velocity vs wave number is shown for layers with perfect bonding, due to shear waves polarized in the x_2-direction and propagating normal to the layering (i.e. in the x_1-direction). Furthermore, the reduction of the shear wave velocity with the imperfect bonding parameter R_t is shown in this figure. The curves predicted by the present theory and those provided by the exact solution given in the Appendix coincide. This forms a direct check to the validity of the model in the present case.

8.2. Harmonic wave propagation normal to long fibers

A fiber-reinforced material with continuous fibers extending in the x_3-direction can be obtained from the present theory in the special case of $l_1/l_2 \to \infty$. Similarly, continuous fibers extending in the x_2-direction are obtained from $h_1/h_2 \to \infty$. In both cases harmonic
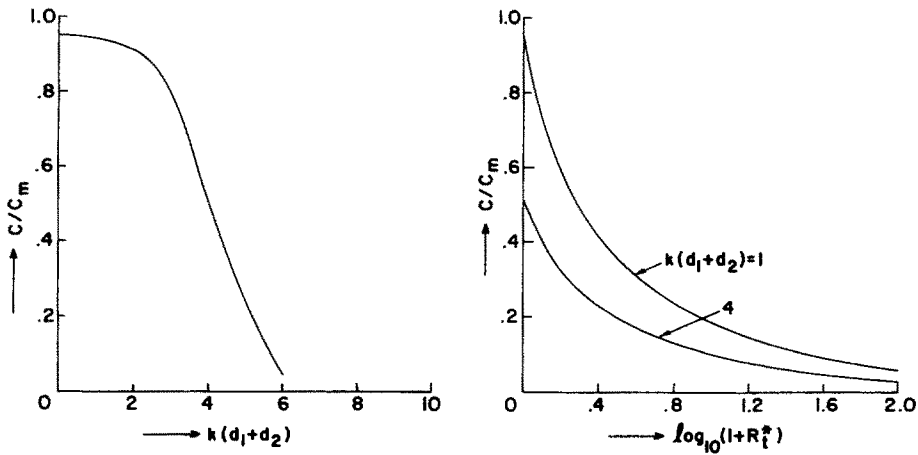
Fig. 3. Phase velocity c/c_m (c_m is the shear wave speed in the matrix) against wave number k for propagating shear waves in a fiber-reinforced material (characterized by eqns (72)) normal to the fibers which extend in the x_3-direction, with perfect contact between the constituents (left). Reduction of phase velocity with debonding in shear parameter $R_t^* = R_t \mu_m/(d_1 + d_2)$ (right).
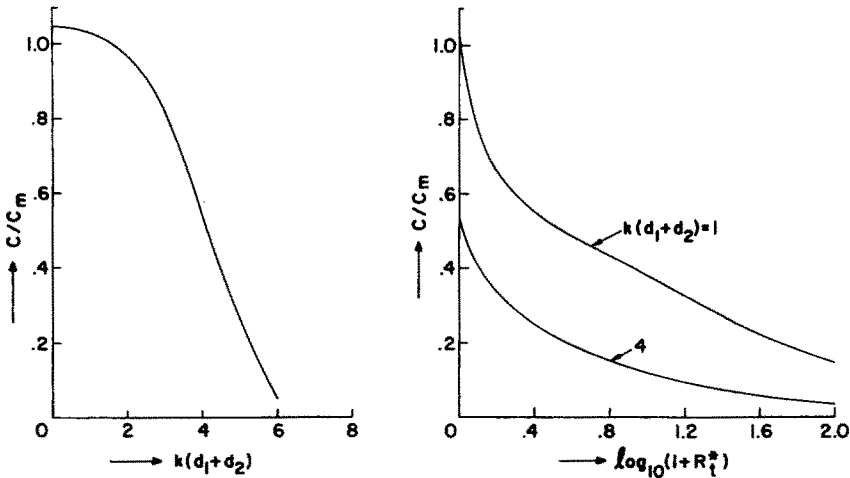

Fig. 4. Same as Fig. 3 but for long fibers extending in the x_2-direction.

shear waves propagating in the x_1-direction give rise to dispersive waves in the composite propagating normal to fibers.

Let the fibers and matrix be isotropic materials with the following constants:

$$\rho_f/\rho_m = 3, \quad \mu_f/\mu_m = 100, \quad v_f = 0.3, \quad v_m = 0.35 \tag{72}$$

where "f" and "m" denote, respectively, the fiber and matrix properties (v stands for Poisson's ratio). The fibers are of square cross-section which are imbedded at equal spacing within the matrix such that the volume ratio is 0.36. In Fig. 3 the phase velocity (normalized with respect to $c_m = (\mu_m/\rho_m)^{1/2}$) is shown against the wave number, for shear waves propagating normal to the fibers. The fibers extend in the x_3-direction and perfect bonding between phases is assumed. On the other hand in the same figure, the deterioration of the phase velocity is shown due to imperfect bonding in shear between the constituents.

In Fig. 4, the resulting phase velocities due to harmonic shear waves propagating in the x_1-direction normal to the fibers which extend this time in the x_2-direction are shown. Both Figs 3 and 4 clearly exhibit the dispersive behavior and the effect of imperfect bonding on the propagating waves.
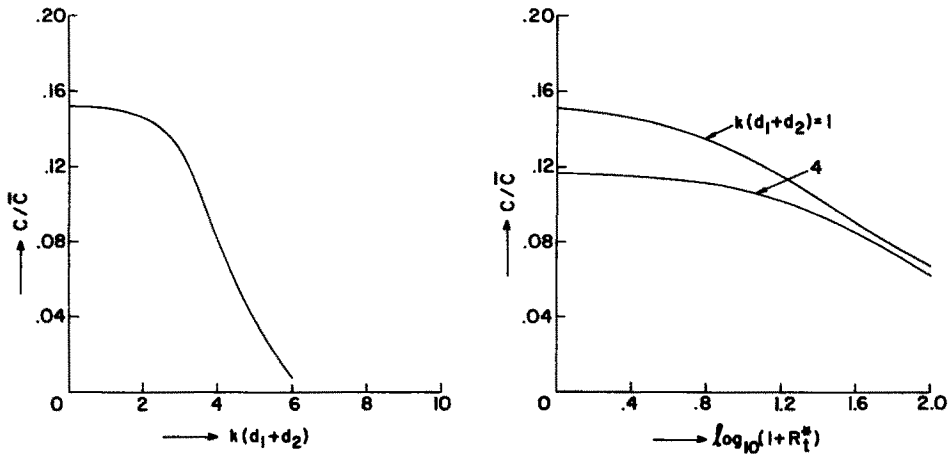
Fig. 5. Phase velocity $c/\bar{c}$ ($\bar{c}$ is the effective wave speed in the composite) against wave number k for propagating shear waves in a short-fiber composite (characterized by eqns (73) and $d_1 + d_2 = h_1 + h_2 = l_1 + l_2$, $d_1/(d_1 + d_2) = 0.8$, $h_1/(h_1 + h_2) = 0.7$, $l_1/(l_1 + l_2) = 0.9$ such that the reinforcement volume ratio is $v_f = 0.504$). The wave propagates in the x_1-direction, polarized in the x_2-direction and perfect contact is assumed between the matrix and inclusions (left). Reduction of phase velocity with debonding parameter in shear $R_t^* = R_t[(\lambda_f + 2\mu_f)v_f + (\lambda_m + 2\mu)(1 - v_f)]/(d_1 + d_2)$ (right).

8.3. Harmonic waves in short-fiber composites

Consider the propagation of shear waves in the x_1-direction, polarized in the x_2-direction, in a composite which consists of fibers of finite dimension (i.e. short-fiber composite). We choose to present dispersion curves and the effect of debonding on phase velocities for a composite with rectangular inclusions. Both matrix and fibers are isotropic with the following material properties:

$$\rho_f/\rho_m = 3, \quad \mu_f/\mu_m = 50, \quad v_f = 0.3, \quad v_m = 0.35. \tag{73}$$

The composite is specified by $d_1 + d_2 = h_1 + h_2 = l_1 + l_2$, $d_1/(d_1 + d_2) = 0.8$, $h_1/(h_1 + h_2) = 0.7$ and $l_1/(l_1 + l_2) = 0.9$ giving a reinforcement volume ratio $v_f = d_1 h_1 l_1/[(d_1 + d_2)(h_1 + h_2) \times (l_1 + l_2)] = 0.504$.

In Fig. 5 the phase velocity vs wave number is presented in the case of perfect bonding. The normalization is with respect to $\bar{c}$ where

$$\bar{c}^2 = \frac{[(\lambda_f + 2\mu_f)v_f + (\lambda_m + 2\mu_m)(1 - v_f)]}{[\rho_f v_f + \rho_m(1 - v_f)]}$$

with $\lambda = \mu/(1 - 2v)$. The validity of this prediction was checked (Aboudi, 1986) with the results of Minagawa and Nemat-Nasser (1976) and good agreement was obtained. In the same figure the decrease of the phase velocity due to imperfect bonding in shear is exhibited.

Next, let us consider a composite the constituents of which are characterized by eqns (73) but the geometrical parameters of which are:

$$d_1 + d_2 = h_1 + h_2 = l_1 + l_2, \quad d_1/(d_1 + d_2) = 0.8,$$

$$h_1/(h_1 + h_2) = 0.9 \quad \text{and} \quad l_1/(l_1 + l_2) = 0.7.$$

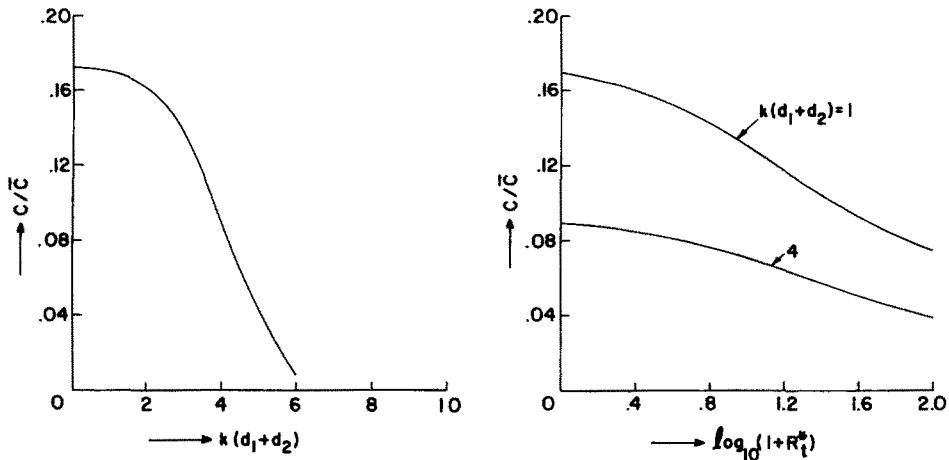The phase velocity for shear waves polarized in the x_2-direction and propagating in this

Fig. 6. Same as Fig. 5 but for the shear waves propagating in the x_1-direction and polarized in the x_3-direction.

Table 1. Elastic constants, mass densities and geometrical parameters of T300-graphite inclusions (transversely isotropic) and epoxy matrix (isotropic). Parameters E_A and v_A denote the axial Young's modulus and Poisson's ratio, G_A denotes the axial shear modulus, E_T and v_T stand for the transverse Young's modulus and Poisson's ratio, and ρ the mass density

	E_A (GPa)	v_A	E_T (GPa)	v_T	G_A (GPa)	ρ (g cm^{-3})
T300-graphite	220	0.3	22	0.35	22	1.72
epoxy	3.45	0.35	3.45	0.35	1.28	1.18

$d_1 = h_1 = l_1 = 0.1$ cm, $v_f = 0.1$.

composite in the x_1-direction is shown in Fig. 6 assuming perfect bonding. Its deterioration with the increase in the parameters of imperfect bonding in shear is exhibited in the same figure. It should be noted that Fig. 6 depicts, equivalently, the propagation of shear waves in the x_1-direction in the previous composite of Fig. 5, but polarized this time in the x_3-direction.

8.4. Transient waves in particulate composites

The present theory can be applied to study the effect of debonding between the phases of a composite material on a propagating pulse. To this end, consider a particulate composite $(d_1 = h_1 = l_1,\ d_2 = h_2 = l_2)$ which consists of an epoxy matrix reinforced by graphite inclusions. The geometrical parameters and material properties of the isotropic matrix and transversely isotropic inclusions are given in Table 1. The orientation of the axis of symmetry of the transversely isotropic graphite is in the x_1-direction. A semi-infinite unit shear stress loading is applied at the surface $x_1 = 0$ (see eqns (59)), while the boundary $x_1 = D$ with $D = 10(d_1 + d_2)$ is kept traction free (see eqns (60)), and the time response of the material is detected at section $x_1 = 2(d_1 + d_2)$. The response exhibits the time variation of the average shear stress at this section and is computed from

$$\bar{\sigma}_{12} = \frac{[v_{211}S^{(211)}_{12(0,0,0)} + v_{212}S^{(212)}_{12(0,0,0)} + V_{221}S^{(211)}_{12(0,0,0)} + v_{222}S^{(222)}_{12(0,0,0)}]}{v_{211} + v_{212} + v_{221} + v_{222}}. \quad (74)$$

In Fig. 7 the average stress is shown against time in the following cases: (a) perfect bonding exists between the matrix and inclusions, (b) perfectly lubricated contact in shear (i.e. $R_n = 0$, $R_t \to \infty$), and (c) complete loss of contact between the phases (i.e. $R_n \to \infty$, $R_t \to \infty$). This latter case corresponds therefore to pulse propagation in a porous epoxy. The figure exhibits well the effect of the interfacial conditions on the response of composite materials.
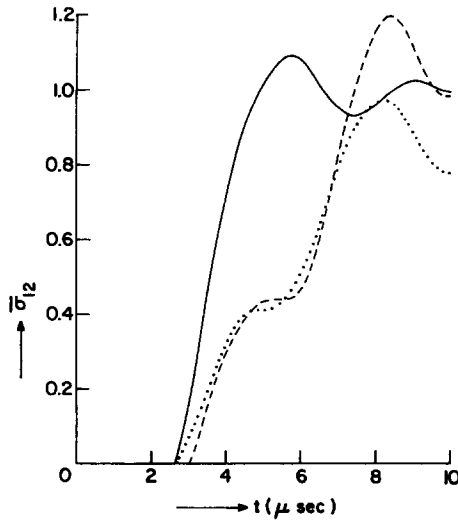
Fig. 7. The variation of the average shear stress, eqn (74), at section $x_1 = 2(d_1+d_2)$ of a particulate graphite/epoxy composite the properties of which are given in Table 1. The stresses are created by a unit semi-infinite impulsive shear loading at the surface $x_1 = 0$ while keeping the surface $x_1 = D = 10(d_1+d_2)$ free of tractions. The solid line (————) exhibits the response when the inclusions are in perfect contact with the matrix, the dashed line (-- -- --) corresponds to perfect lubrication, and the dotted line (· · · ·) for porous epoxy.
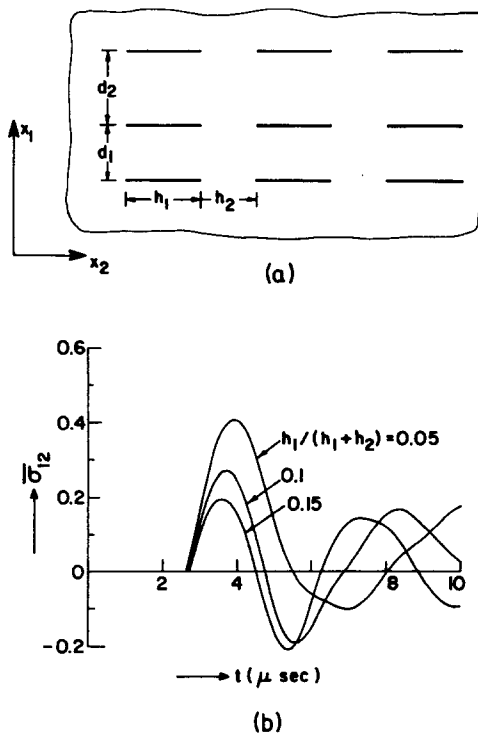

(a)

(b)

Fig. 8. (a) Solid with periodically spaced cracks. (b) Time variation of the average shear stress, eqn (74), at section $x_1 = 2(d_1+d_2)$ of a cracked epoxy matrix. The stresses are created by a unit semi-infinite impulsive shear loading at the surface $x_1 = 0$, while keeping the surface $x_1 = D = 10(d_1+d_2)$ traction free. The geometrical parameters are $d_1 = d_2 = 0.1$ cm and $h_1+h_2 = 0.2$ cm.

8.5. Wave propagation in a solid with a periodic distribution of cracks

Let us apply the derived continuum theory for the prediction of the response of a material containing cracks which are distributed in periodic arrays (Fig. 8(a)). This two-dimensional situation can be obtained as a special case from the general configuration of Fig. 1(a) by filling the inclusions with the same material as that of the matrix and imposing

complete debonding between subcells ($\alpha = 1, \beta = 1, \gamma = 1$) and ($\alpha = 2, \beta = 1, \gamma = 1$), and ($\alpha = 1, \beta = 1, \gamma = 2$) and ($\alpha = 2, \beta = 1, \gamma = 2$).

Let a semi-infinite shear stress loading, eqns (59), of a unit amplitude be applied at the surface $x_1 = 0$, while the surface $x_1 = D$, with $D = 10(d_1 + d_2)$, is kept traction free (6), and the time response of the cracked material is computed at section $x_1 = 2(d_1 + d_2)$. In Fig. 8(b) the resulting average shear stress $\bar{\sigma}_{12}$ (given by eqn (74)) is shown for a cracked epoxy matrix with $d_1 = d_2 = 0.1$ cm and $h_1 + h_2 = 0.2$ cm. The time response is exhibited for several values of crack spacing in the x_2-direction. The effect of the cracks on the propagating pulse, which would simply be a propagating unit step function in the uncracked solid, is clearly seen.

The present continuum theory can also be utilized to investigate the propagation of harmonic waves in the solid with a periodic distribution of cracks. In a recent publication by Achenbach and Li (1986), an exact solution for the propagation of horizontally polarized harmonic transverse waves in a solid with periodic cracks is given. Since the anti-plane waves propagate in the normal direction of the cracks, we can conform the general configuration of Fig. 1(a) to the two-dimensional problem of Achenbach and Li by considering shear waves propagating in the x_1-direction and polarized in the x_2-direction such that expansion (5) is applicable (Fig. 9(a)). The inclusion and matrix materials are identical, but complete debonding is imposed between subcells ($\alpha = 1, \beta = 1, \gamma = 1$) and ($\alpha = 2, \beta = 1, \gamma = 1$), as well as between subcells ($\alpha = 1, \beta = 2, \gamma = 1$) and ($\alpha = 2, \beta = 2, \gamma = 1$).

In Fig. 9(b) the circular frequency $\omega d_1/c_m$ (c_m is the shear wave speed in the uncracked material) is shown vs wave number. The figure exhibits a comparison between the result provided by the present continuum model and the exact solution of Achenbach and Li (1986), and the agreement is reasonable. It should be noted that the present approach can
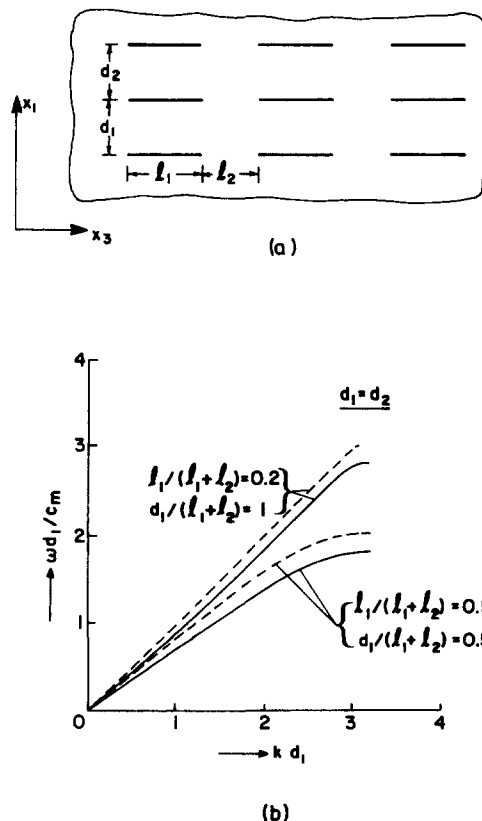

(a)

(b)

Fig. 9. (a) Solid with periodically spaced cracks. (b) Circular frequency against wave number for shear waves oriented in the x_2-direction and propagating in the x_1-direction in the cracked solid (c_m is the shear wave speed in the uncracked material). Solid lines (——) present theory, dashed lines (- - - -) exact solution.

be applied to other types of harmonic waves for which exact solutions may be difficult and unknown.

8.6. Transient waves in damaged composite laminates

It is well known that transverse-ply cracking appears in composite laminates subjected to either a quasi-static or cyclic loading. In Fig. 10(a) a section of a cross-ply laminate is shown with the transverse cracks extending from edge to edge in the fiber direction (x_3-direction) and across the thickness of the $90°$ plies. The periodic distribution of the transverse cracks in the $90°$ ply is well established, see Highsmith and Reifsnider (1982) for example.

The present continuum model can be applied to investigate the influence of the existence of the transverse cracks in a cross-ply laminate on the propagation of waves in the composite laminate. The general configuration of Fig. 1(a) can be adjusted to conform to the cracked cross-ply laminate of Fig. 10(a) by filling the subcells ($1\beta\gamma$) with a unidirectional fiber-reinforced material with fibers aligned in the x_2-direction. The subcells ($2\beta\gamma$) are filled with the same material but with fibers oriented in the x_3-direction. In addition, complete debonding (in normal and shear) is imposed between subcells ($\alpha = 2$, $\beta = 1$, $\gamma = 1$) and ($\alpha = 2$, $\beta = 2$, $\gamma = 1$), and between ($\alpha = 2$, $\beta = 1$, $\gamma = 2$) and ($\alpha = 2$, $\beta = 2$, $\gamma = 2$).

We choose a glass/epoxy cross-ply laminate the ply material properties of which are given in Table 2, with $d_1 = d_2 = 0.0203$ cm (Highsmith and Reifsnider, 1982). A semi-infinite shear stress loading of unit amplitude is applied at the surface $x_1 = 0$ (eqns (59)) while the boundary surface $x_1 = D$ ($D = 5(d_1 + d_2)$) is kept traction free (eqns (60)). The response is detected at section $x_1 = 3(d_1 + d_2)$ where the average stress $\bar{\sigma}_{12}$ (eqn (74)) is computed. In Fig. 10(b) a comparison between propagating stress waves is shown for
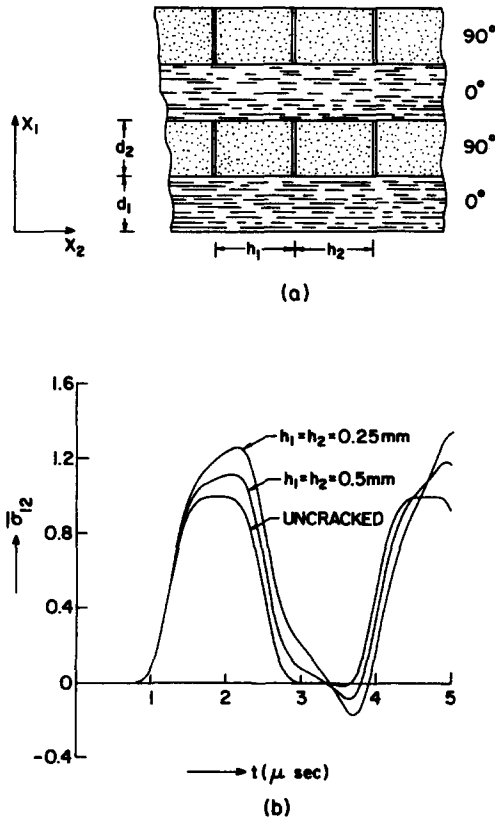

(a)

(b)

Fig. 10. (a) A section of a cross-ply composite laminate with transverse cracks at the $90°$ plies. (b) Time variation of the average shear stress, eqn (74), at section $x_1 = 3(d_1 + d_2)$ of cracked and uncracked cross-ply laminates, caused by a unit semi-infinite impulsive shear stress loading at $x_1 = 0$, while the surface $x_1 = 5(d_1 + d_2)$ is kept traction free. The properties of the glass/epoxy layers are given in Table 2, and $d_1 = d_2 = 0.0203$ cm.

Table 2. Elastic constants of a unidirectional glass/epoxy (uncracked) solid. Parameters E_A and v_A denote the axial Young's modulus and Poisson's ratio, G_A denotes the axial shear modulus, E_T and v_T stand for the transverse Young's modulus and Poisson's ratio, and ρ the mass density

E_A (GPa)	v_A	E_T (GPa)	v_T	G_A (GPa)	ρ (g cm^{-3})
41.7	0.3	13	0.42	3.4	1.8

two types of cracked laminates together with the corresponding propagating wave in the uncracked laminate (in which perfect bonding exists between all interfaces). The significant effect of the transverse cracks on the propagating pulses is clear.

In addition to the transverse cracks which appear in a composite laminate at the earlier stage of loading, longitudinal cracks appear in a later stage along the fibers in the $0°$ ply (Jamison et al., 1984). In Fig. 11(a) a cross-ply laminate is shown in which transverse cracks as well as longitudinal cracks exist. The present theory can be applied to the present situation to study the influence of these systems of matrix cracks on a propagating pulse in the damaged laminate.

The general configuration of Fig. 1(a) can be conformed to the cracked laminate of Fig. 11(a) by filling the subcells $(1\beta\gamma)$ with a unidirectional composite with fibers oriented in the x_2-direction, while the subcells $(2\beta\gamma)$ are filled with the same material but with fibers in the x_3-direction. The existence of the transverse and longitudinal cracks is simulated by imposing complete debonding between subcells $(\alpha = 2, \beta = 1, \gamma = 1)$ and $(\alpha = 2, \beta = 2,$
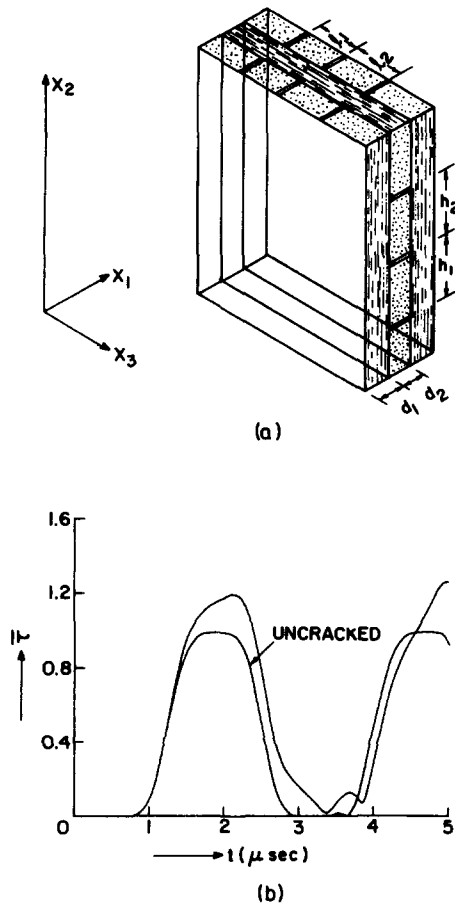

(a)

(b)

Fig. 11. (a) A section of a cross-ply composite laminate with transverse and longitudinal cracks. (b) Time variation of the resultant shear stress $\bar{\tau}$ at section $x_1 = 3(d_1 + d_2)$ of the uncracked and cracked cross-ply laminates, caused by unit semi-infinite impulsive stresses $\sigma_{12}^{(1\beta\gamma)}$ and $\sigma_{13}^{(1\beta\gamma)}$ applied at $x_1 = 0$, while the rear surface $x_1 = 5(d_1 + d_2)$ is kept traction free. The properties of the glass/epoxy plies are given in Table 2, and $d_1 = d_2 = 0.0203$ cm, $h_1 = h_2 = 0.025$ cm, $l_1 = l_2 = 0.05$ cm.

$\gamma = 1$), ($\alpha = 2$, $\beta = 1$, $\gamma = 2$) and ($\alpha = 2$, $\beta = 2$, $\gamma = 2$), ($\alpha = 1$, $\beta = 1$, $\gamma = 1$) and ($\alpha = 1$, $\beta = 1$, $\gamma = 2$), and ($\alpha = 1$, $\beta = 2$, $\gamma = 1$) and ($\alpha = 1$, $\beta = 2$, $\gamma = 2$).

The same glass/epoxy cross-ply laminate is chosen as before with the ply properties given in Table 2, and $d_1 = d_2 = 0.0203$ cm, $h_1 = h_2 = 0.025$ cm, $l_1 = l_2 = 0.05$ cm. In order to take into account the simultaneous effects of the two types of cracks, two semi-infinite shear loadings $\sigma_{12}^{(1\beta\gamma)}$ and $\sigma_{13}^{(1\beta\gamma)}$ each of unit amplitude, are applied at the surface $x_1 = 0$, while the rear surface at $x_1 = 5(d_1+d_2)$ is kept traction free. The resulting pulse will be traveling in the x_1-direction and polarized in the 45° direction of the (x_2, x_3) plane. In Fig. 11(b) the resultant shear stress $\bar{\tau} = [\frac{1}{2}(\bar{\sigma}_{12}^2+\bar{\sigma}_{13}^2)]^{1/2}$ computed at $x_1 = 3(d_1+d_2)$ is shown together with the corresponding one traveling in the undamaged laminate. The two curves exhibit well the combined influence of transverse and longitudinal cracks on a propagating pulse in the cross-ply laminate.

REFERENCES

Aboudi, J. (1986). Harmonic waves in composite materials. *Wave Motion* **8**, 289–303.
Aboudi, J. (1987a). Transient waves in composite materials. *Wave Motion* **9**, 141–156.
Aboudi, J. (1987b). Damage in composites: modeling of imperfect bonding. *Compos. Sci. Technol.* **28**, 103–128.
Achenbach, J. D. and Li, Z. L. (1986). Propagation of horizontally polarized transverse waves in a solid with a periodic distribution of cracks. *Wave Motion* **8**, 371–379.
Christensen, R. M. (1979). *Mechanics of Composite Materials*. Wiley-Interscience, New York.
Highsmith, A. L. and Reifsnider, K. L. (1982). Stiffness-reduction mechanisms in composite laminates. *ASTM STP* **775**, 103–117.
Jamison, R. D., Schulte, K., Reifsnider, K. L. and Stinchcomb, W. W. (1984). Characterization and analysis of damage mechanisms in tension—tension fatigue of graphite/epoxy laminates. *ASTM STP* **836**, 21–55.
Jones, J. P. and Whittier, J. S. (1967). Waves at a flexibly bonded interface. *J. Appl. Mech.* **34**, 905–909.
Minagawa, S. and Nemat-Nasser, S. (1976). Harmonic wave in three-dimensional elastic composites. *Int. J. Solids Structures* **12**, 769–777.
Sun, C. T., Achenbach, J. D. and Herrmann, G. (1968). Continuum theory for a laminated medium. *J. Appl. Mech.* **35**, 467–475.
Theocaris, P. S. and Phillippidis, T. P. (1985). Theoretical evaluation of the extent of the mesophase in particulate and fibrous composites. *J. Reinf. Plastics Composites* **4**, 173–185.
Thompson, R. B. (1984). Application of elastic wave scattering theory to the detection and characterization of flaws in structural materials. In *Wave Propagation in Homogeneous Media and Ultrasonic Nondestructive Evaluation*, AMD-Vol. 62, pp. 61–73. Am. Soc. Mech. Engrs, New York.

APPENDIX: DISPERSION RELATION FOR A PERIODICALLY LAYERED MEDIUM WITH IMPERFECT BONDING

Consider a periodic array of two alternating homogeneous and isotropic layers with thickness d_1 and d_2. Imperfect bonding exists between the layers which is given by eqns (1)–(3). The dispersion relations of this laminated composite can be obtained from the general development given in this paper in the special case of $h_1/h_2 \to \infty$ and $l_1/l_2 \to \infty$ (Fig. 1(a)). It is possible, on the other hand, to derive these relations directly from the elastodynamic equations in an exact manner. These relations can be used to check the validity of prediction of the proposed continuum approach, and it turns out that the phase velocities provided by the two approaches coincide. This forms a direct check of the proposed model in the present situation.

In a homogeneous isotropic elastic material the scalar and vector displacement potentials satisfy

$$\nabla^2 \psi = \ddot{\psi}/c_L^2, \quad \nabla^2 \mathbf{H} = \ddot{\mathbf{H}}/c_T^2 \tag{A1}$$

where $c_L^2 = (\lambda+2\mu)/\rho$, $c_T^2 = \mu/\rho$ with λ, μ being the Lamé constants of the material and ρ its mass density. The displacement is given by

$$\mathbf{u} = \operatorname{grad} \psi + \operatorname{rot} \mathbf{H}. \tag{A2}$$

To study longitudinal waves propagating in the direction normal to the layering (e.g. x_2-direction), we allocate, for convenience, the origin of the coordinate system at the interface plane of one pair of layers. For the two types of layers, labeled with $\alpha = 1, 2$, solutions for the scalar potential are sought of the form

$$\psi^{(\alpha)} = \Psi^{(\alpha)}(x_2) \exp [ik(x_2-ct)]. \tag{A3}$$

Solving the wave equation we find

$$\Psi^{(\alpha)} = A_\alpha \exp\left[-ik\left(1+\frac{c}{c_L^{(\alpha)}}\right)x_2\right] + B_\alpha \exp\left[-ik\left(1-\frac{c}{c_L^{(\alpha)}}\right)x_2\right]. \qquad (A4)$$

The displacement components $u_2^{(\alpha)}$ are obtained from eqn (A2) in the form

$$u_2^{(\alpha)} = ik\frac{c}{c_L^{(\alpha)}}\left[-A_\alpha \exp\left(-ik\frac{c}{c_L^{(\alpha)}}x_2\right) + B_\alpha \exp\left(ik\frac{c}{c_L^{(\alpha)}}x_2\right)\right]\exp\left(-ikct\right). \qquad (A5)$$

The non-trivial stresses follow from

$$\sigma_{22}^{(\alpha)} = (\lambda_\alpha + 2\mu_\alpha)\frac{\partial u_2^{(\alpha)}}{\partial x_2}. \qquad (A6)$$

In view of periodicity, $\Psi^{(\alpha)}$ are periodic with period $d_1 + d_2$. The four constants A_α, B_α are determined from the following conditions at the interfaces within the pair of layers p, and between the pair p and $p+1$:

$$\sigma_{22}^{(1)}|^{(p)} = \sigma_{22}^{(2)}|^{(p)}, \qquad x_2 = 0$$
$$\sigma_{22}^{(1)}|^{(p+1)} = \sigma_{22}^{(2)}|^{(p)}, \qquad x_2 = d_2$$
$$u_2^{(1)}|^{(p)} - u_2^{(2)}|^{(p)} = -R_n\sigma_{22}^{(1)}|^{(p)}, \qquad x_2 = 0$$
$$u_2^{(1)}|^{(p+1)} - u_2^{(2)}|^{(p)} = R_n\sigma_{22}^{(1)}|^{(p+1)}, \qquad x_2 = d_2.$$

The frequency equation is obtained as a condition for the vanishing of the following determinant:

$$\det[\mathbf{D}] = 0 \qquad (A7)$$

where $\mathbf{D}$ is a 4×4 matrix the elements of which are

$$D_{11} = D_{12} = \rho_1$$
$$D_{13} = D_{14} = -\rho_2$$
$$D_{21} = -\rho_1 \exp(i\xi)E_{1p}$$
$$D_{22} = -\rho_1 \exp(i\xi)E_{1m}$$
$$D_{23} = \rho_2 E_{2m}$$
$$D_{24} = \rho_2 E_{2p}$$
$$D_{31} = -ikc/c_L^{(1)} - R_n\rho_1 k^2 c^2$$
$$D_{32} = ikc/c_L^{(1)} - R_n\rho_1 k^2 c^2$$
$$D_{33} = ikc/c_L^{(2)}$$
$$D_{34} = -D_{33}$$
$$D_{41} = -i\exp(i\xi)E_{1p}kc/c_L^{(1)}$$
$$D_{42} = i\exp(i\xi)E_{1m}kc/c_L^{(1)}$$
$$D_{43} = ikc\,E_{2m}/c_L^{(2)} + R_n\rho_2 k^2 c^2 E_{2m}$$
$$D_{44} = -ikc\,E_{2p}/c_L^{(2)} + R_n\rho_2 k^2 c^2 E_{2p}$$

with

$$\xi = k(d_1 + d_2), \quad E_{\alpha p} = \exp(ikcd_\alpha/c_L^{(\alpha)}), \quad E_{\alpha m} = \exp(-ikcd_\alpha/c_L^{(\alpha)}).$$

It can be verified that eqn (A7) reduces in the case of perfect bonding ($R_n = 0$) to the frequency equation given by Sun et al. (1968) (eqn (99)).

The analysis for transverse waves propagating in the direction normal to the layering is very similar. It may be verified that the dispersion relation is still given by eqn (A7) provided that $c_L^{(\alpha)}$ is replaced by $c_T^{(\alpha)}$ and R_n by R_t.